Simple analysis method for determining internal quantum efficiency and relative recombination ratios in light emitting diodes

Yang-Seok Yoo,[1,a)] Tae-Moo Roh,[1,a)] Jong-Ho Na,[2] Sung Jin Son,[2] and Yong-Hoon Cho[1,b)]
[1]*Department of Physics, Graduate School of Nanoscience & Technology (WCU), KAIST Center for LED Research, and KI for the NanoCentury, KAIST, Daejeon 350-701, South Korea*
[2]*LG Innotek, LED Division, LED R&D Center, Paju 413-901, South Korea*

(Received 2 April 2013; accepted 6 May 2013; published online 30 May 2013)

We propose a facile analysis method for determining internal quantum efficiency (IQE) and relative carrier recombination ratios in light emitting diodes (LEDs). Using this method, IQE and different contributions of radiative and nonradiative recombination processes at arbitrary excitation power can be unambiguously determined without any knowledge of A, B, and C coefficients of the rate equation. We applied our analysis method to two LED samples grown on different substrates with distinct material quality and found good agreement with experimental results such as ω-rocking curve obtained by high resolution x-ray diffraction and decay lifetime measured by time-resolved photoluminescence. © *2013 AIP Publishing LLC*. [http://dx.doi.org/10.1063/1.4807485]

Recently, GaN-based high-power light emitting diodes (LEDs) have been widely utilized in advanced technologies, such as automotive headlights, indoor/outdoor lighting, back-lighting, and display. LEDs, in principle, are capable of generating white light with a 20 times greater efficiency than incandescent light sources.[1] However, GaN-based high-power LEDs suffer from a phenomenon known as efficiency droop, i.e., a reduction of the external quantum efficiency (EQE) with increasing injection current; the physical origin of the droop is still under intense debate.[2] Typical GaN-based LEDs exhibit a peak efficiency at current densities as low as 0.1-10 A/cm^2,[3] above which efficiency gradually decreases. The EQE of an LED is defined as the product of the internal quantum efficiency (IQE) and the light extraction efficiency (LEE). The former is related to the crystal quality and structure of the epitaxial layer, while the latter is associated with chip processing, die geometry, and LED packaging. The decrease in EQE with injection current is generally attributed to a reduction of IQE, since LEE is usually constant with injection current. Several groups have shown that IQE experimentally and theoretically depends on injection current.[2,4,5] Therefore, extracting out IQE and related recombination information from experimental data becomes very important to investigate and eventually overcome the efficiency droop occurring in high-power LEDs.

However, the calculation of IQE is quite difficult due to complicated measurement and a lack of theories. Previously, the IQE of compound semiconductors has been determined using several proposed experimental methods and theoretical models, such as absolute intensity measurements using an integrating sphere,[6] steady-state thermal study,[7] time-resolved photoluminescence (PL),[8] temperature-dependent measurement,[9] and the semiconductor rate equation.[10] However, these methods to measure IQE provide less accurate results for IQE due to their ambiguous assumptions. For example, the experimental approach using PL measurement usually assumes the value of IQE at low temperature to be unity. In addition, an arbitrary value of the radiative recombination coefficient B (e.g., in the range of 10^{-10}–10^{-11} cm^3 s^{-1}) has typically been chosen in the conventional rate equation, and therefore the same radiative recombination lifetime, which is inversely proportional to B, is expected regardless of the sample structure at the same excitation condition. However, this assumption often leads to controversy since the radiative recombination lifetime observed experimentally can be different in practice depending on the sample's material condition and structure (i.e., according to indium composition and well width).[11,12]

Recently, the idea that the conventional rate equation, often referred to as the ABC model, using *constant* A, B, and C coefficients may no longer be suitable to explain efficiency droop behavior, has been widely discussed. Several modified ABC models using *non-constant* A, B, and C coefficients (i.e., these values are functions of carrier density n) have been proposed that consider density-activated defect recombination,[13] phase-space filling,[14] the internal field screening effect,[15] etc. Furthermore, the C coefficient (i.e., n^3 dependence) can be associated with the Auger process and/or the carrier overflow process, and even higher terms (e.g., the D coefficient for n^4 dependence or higher) related to carrier overflow can be needed for better fitting of the experimental data.[16] As described above, in fact, there are multiple ways to fit and explain the *same* experimental data based on *different* models and assumptions. Nevertheless, it is still very useful if one can analyze the different dependences of n associated with various possible recombination processes in the ABC model and directly connect those dependences to measurable quantities. Furthermore, in order to investigate and improve device performance, information about IQE and the relative ratios between radiative to nonradiative recombination processes can be more important and practical, instead of determining A, B, and C coefficients using many assumptions.

In this work, we proposed a simple analysis method for IQE extraction from excitation power-dependent PL data based on the simplified ABC rate equation. Our method does not require any knowledge or assumption about the values of

[a)]Y.-S. Yoo and T.-M. Roh contributed equally to this work.
[b)]Electronic mail: yhc@kaist.ac.kr

A, B, and C coefficients, unlike the case of conventional rate equation. Furthermore, our method allows us to analyze the relative ratios of various radiative and nonradiative recombination processes, which are in good agreement with our experimental data. For comparison, we applied this method for InGaN/GaN multiple quantum well (MQW) grown on two different substrates.

Our proposed model is based on the rate equation, which is the relationship between total carrier generation rate (G) and individual recombination rate

$$G = An + Bn^2 + Cn^3. \tag{1}$$

The three main carrier recombination mechanisms in the rate equation are Shockley-Read-Hall (SRH) nonradiative recombination (An), radiative recombination (Bn^2), and Auger (and/or possibly carrier overflow) nonradiative recombination (Cn^3), in which A, B, and C are the respective recombination coefficients and n is the carrier concentration. IQE (η) is defined as the radiative recombination rate over the total carrier generation rate

$$\eta = \frac{Bn^2}{An + Bn^2 + Cn^3}. \tag{2}$$

Contrary to the model using the conventional rate equation, our proposed model uses the relation between the integrated PL intensity (I_{PL}) and G

$$I_{PL} = aBn^2, \tag{3}$$

$$G = A\sqrt{\frac{I_{PL}}{aB}} + \frac{I_{PL}}{a} + \frac{C{I_{PL}}^{3/2}}{[aB]^{3/2}}, \tag{4}$$

where a is a constant determined by the volume of the excited active region and the total collection efficiency of luminescence. The relationship between laser excitation power (P_{laser}) and G is expressed as

$$G = xP_{laser}, \tag{5}$$

$$x = \frac{(1-R)\alpha}{A_{spot}h\nu}, \tag{6}$$

where R is the Fresnel reflection at the sample surface, α is the absorption coefficient of the active region, A_{spot} is the area of the laser spot on the LED sample, and $h\nu$ is the photon energy of the excitation laser. We used identical values of a and x for our samples since the experimental conditions and the sample structures are the same, except for that of the substrate. Therefore, Eqs. (4) and (5) can be expressed as follows:

$$P_{laser} = \frac{A}{x\sqrt{aB}}\sqrt{I_{PL}} + \frac{1}{xa}I_{PL} + \frac{C}{x[aB]^{3/2}}{I_{PL}}^{3/2}. \tag{7}$$

In this formula, the terms $\frac{A}{x\sqrt{aB}}$, $\frac{1}{xa}$, and $\frac{C}{x[aB]^{3/2}}$ can be changed using the fitting parameters P_1, P_2, and P_3, respectively, from the power-dependence PL experiments; thus, Eq. (7) simply becomes

$$P_{laser} = P_1\sqrt{I_{PL}} + P_2I_{PL} + P_3{I_{PL}}^{3/2}. \tag{8}$$

Therefore, η can be directly calculated as follows:

$$\eta = \frac{Bn^2}{G} = \frac{aBn^2}{(xa)P_{laser}} = \frac{I_{PL}P_2}{P_{laser}}. \tag{9}$$

Therefore, in order to calculate IQE, we only need to know the excitation power (P_{laser}), the integrated PL intensity (I_{PL}), and a fitting parameter P_2, which can be obtained easily from the excitation power-dependence PL data, without knowing or assuming other parameters.

In order to apply our analysis method to practical LED devices, we chose InGaN/GaN MQWs grown on patterned sapphire (PAT) and planar sapphire (PLA) substrates (referred to as MQW-on-PAT and MQW-on-PLA, respectively). The MQW-on-PAT is known to have better material quality and consequently higher quantum efficiency than those characteristics of the MQW-on-PLA.[12] The InGaN/GaN MQWs were grown by metal-organic chemical vapor deposition (MOCVD) on c-plane PAT and PLA substrates. After depositing a low-temperature GaN nucleation layer on the substrate, a 5.3-μm-thick n-type GaN:Si layer followed by the InGaN/GaN MQWs was grown. A p-type $Al_{0.2}Ga_{0.8}N$ electron blocking layer and a 60-nm-thick p-type GaN:Mg were deposited on the InGaN/GaN MQWs. Both the MQW-on-PLA and MQW-on-PAT samples are identical in structure, with the exception of the substrates. A continuous-wave 405 nm line laser was chosen as the PL excitation source; the laser energy corresponds to the energy between the band gaps of the InGaN well and the GaN barrier, and therefore excited only in the active layer, not in the n-GaN or p-GaN layers. In order to vary the carrier concentration in the active layer, the laser excitation power was tuned from 0.1 mW to 25 mW using a neutral density filter. We note that in order to apply our proposed method to practical LED devices as a demonstration, we tried in this work to mitigate other unwanted recombination processes by using the moderate excitation power range before reaching the IQE maximum and the excitation energy below the bandgap of the barrier material, which will minimize carrier overflow, heating, and carrier spillover effects in the MQWs.

Figures 1(a) and 1(b) show PL spectra of MQW-on-PAT and MQW-on-PLA with varying of excitation power measured at 15 K, respectively. The emission peak wavelengths are located between 440 and 445 nm and the overall PL intensity, taken from QW emission, increases as the excitation power is increased. The integrated PL intensity I_{PL} of MQW-on-PAT is 58% higher than that of MQW-on-PLA at the maximum excitation power of 25 mW. Experimental data of P_{laser} versus normalized I_{PL} are plotted in Figs. 1(c) and 1(d); these data were obtained from the PL spectra shown in Figs. 1(a) and 1(b), respectively. The fitting results (red lines) based on Eq. (8) are also shown in Figs. 1(c) and 1(d), from which we were able to extract the fitting parameters: P_1 (3.49), P_2 (20.6), and P_3 (1.08) for MQW-on-PAT and P_1 (5.45), P_2 (16.9), and P_3 (2.75) for MQW-on-PLA.

Figure 2 shows the plots of IQE versus P_{laser} for MQW-on-PAT and MQW-on-PLA; these values were extracted

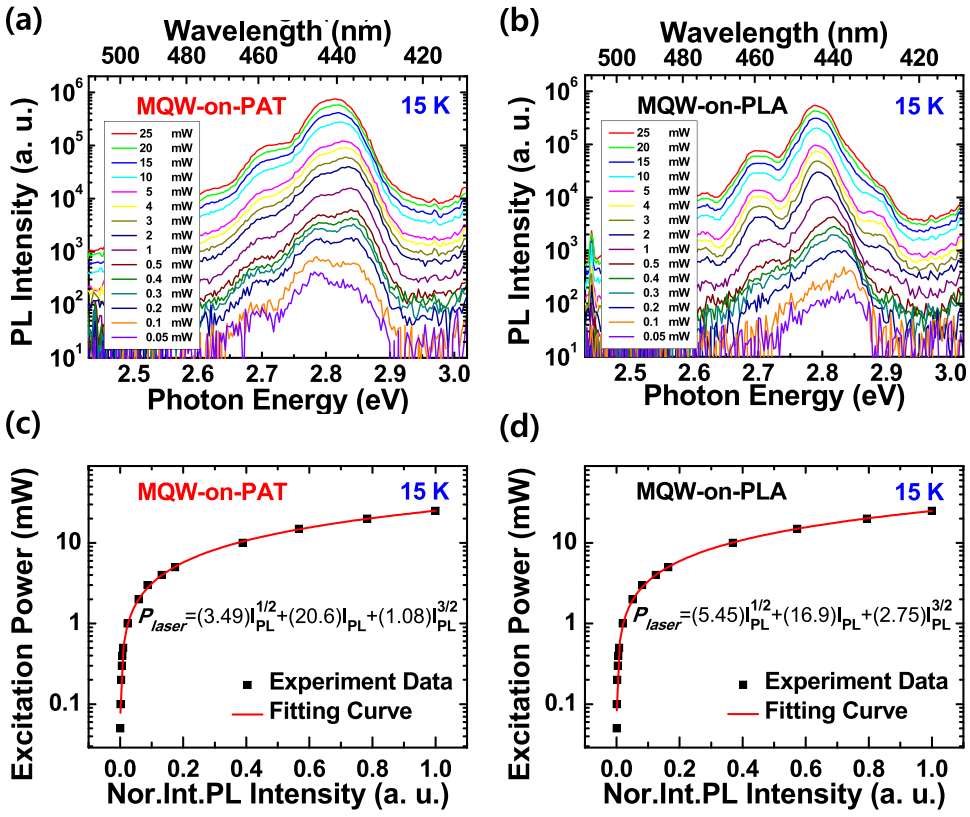

FIG. 1. (a), (b) PL Spectra of InGaN/GaN MQWs and (c), (d) integrated PL intensity (black closed square) as a function of excitation power at low temperature (15 K) and fitted curve (red line) obtained using Eq. (8).

using Eq. (9). We found that, with excitation power, the IQE of MQW-on-PAT increases faster than that of MQW-on-PLA and the overall IQE values of MQW-on-PAT are higher than those of MQW-on-PLA. At the highest excitation power condition (25 mW), the IQEs calculated using Eq. (9) are 82% and 68% for MQW-on-PAT and MQW-on-PLA, respectively. These results reflect the facts that the overall optical properties of MQW-on-PAT are better than those of MQW-on-PLA. Any kind of loss mechanism produces a slower increase in the number of emitted photons as the excitation power increases, resulting in a reduced IQE for low quality materials under certain excitation condition.[17] We also note that degradation of IQE (i.e., efficiency droop) with excitation power was not observed in either sample within our experimental conditions, since the excitation power density is not sufficiently high for the occurrence of dominant Auger effect and the excitation photon energy is chosen to be lower than the band gap of the GaN barriers minimizing the carrier overflow.

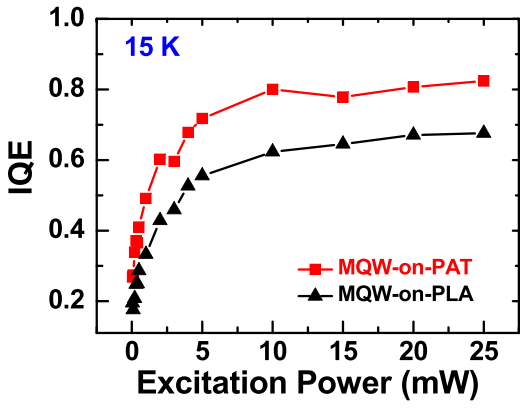

FIG. 2. Comparison of IQE between MQW-on-PAT and MQW-on-PLA as a function of excitation power measured at low temperature (15 K).

Furthermore, we analyzed the ratio between different carrier recombination processes using our fitting parameters as follows:

$$P_1\sqrt{I_{PL}} : P_2 I_{PL} : P_3 {I_{PL}}^{3/2}. \tag{10}$$

The three components of Eq. (10) are the ratio of Shockley-Read-Hall recombination (An), the radiative recombination (Bn^2), and the Auger recombination (and/or carrier overflow) (Cn^3). Figure 3 shows total nonradiative recombination efficiency $(P_1 \cdot {I_{PL}}^{1/2} + P_3 \cdot {I_{PL}}^{3/2})/P_{\text{Laser}}$ and radiative recombination efficiency, $P_2 \cdot I_{PL}/P_{\text{Laser}}$ as a function of excitation power. The MQW-on-PAT sample exhibits smaller $(P_1 \cdot {I_{PL}}^{1/2} + P_3 \cdot {I_{PL}}^{3/2})/P_{\text{Laser}}$ and larger $P_2 \cdot I_{PL}/P_{\text{Laser}}$ compared to the MQW-on-PLA sample. Within our experimental conditions, both samples are dominated by the radiative recombination process instead of nonradiative recombination processes, as shown in Fig. 3(a), except when there are very low excitation power conditions. Moreover, we analyzed the characteristics of the radiative recombination process and the nonradiative recombination processes before the saturation region of IQE [Fig. 3(b), dotted region of Fig. 3(a)]. We found that the cross-over between radiative and nonradiative recombination efficiencies for the MQW-on-PAT sample occurs at a much lower excitation power than that of the MQW-on-PLA sample. It is known that GaN-based layers grown on PAT reveal not only a reduction of dislocation density but also a relaxation of residual strain (and possibly a strain-induced piezoelectric field as well) because of the lateral growth mode during the growth procedure.[18] Therefore,

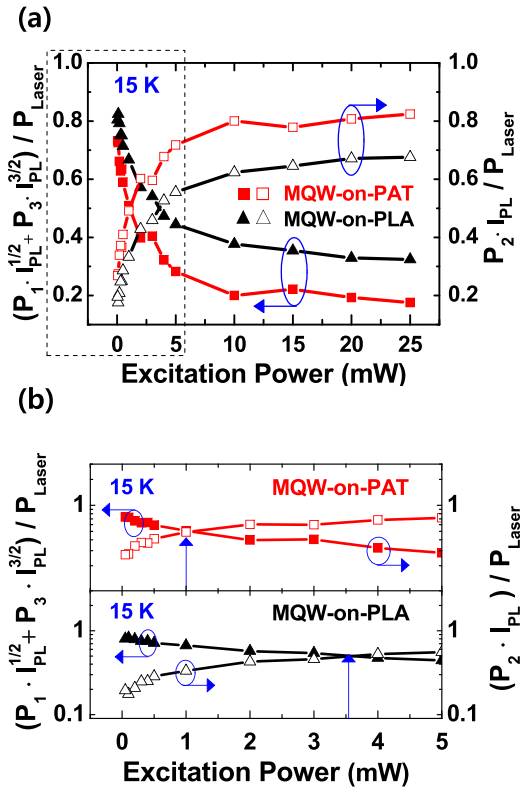

FIG. 3. (a) Variation of radiative ($P_2 \cdot I_{PL}/P_{Laser}$) and total nonradiative ($(P_1 \cdot {I_{PL}}^{1/2} + P_3 \cdot {I_{PL}}^{3/2})/P_{Laser}$) recombination efficiencies with excitation power for MQW-on-PAT and MQW-on-PLA at low temperature (15 K). (b) Radiative and total nonradiative recombination efficiencies in the low excitation power range [i.e., enlarged part of dotted square of Fig. 3(a)].

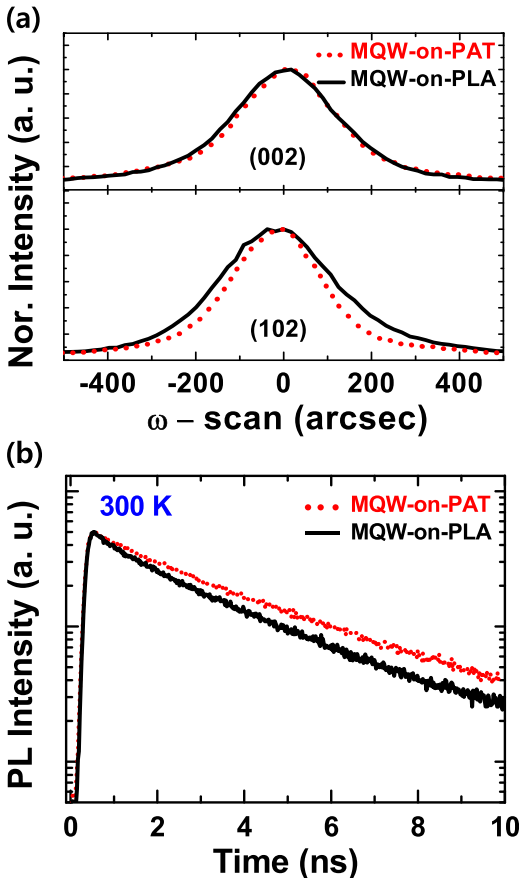

FIG. 4. (a) Symmetric (002) and asymmetric (102) reflection X-ray ω-scan rocking curves measurement. (b) Recombination lifetimes from the InGaN MQWs grown on PAT and PLA substrates measured at room-temperature.

the former results in better material quality and consequently lower nonradiative recombination rate, while the latter leads to enhanced electron-hole wavefunction overlap and hence a higher radiative recombination rate for MQW-on-PAT compared to the case of MQW-on-PLA.[19] These results are in excellent agreement with our observations.

In order to further elucidate and compare the material quality of MQW-on-PAT and MQW-on-PLA, measurements of a ω-scan rocking curve of high resolution X-ray diffraction (HRXRD) and a decay curve of time-resolved PL (TRPL) were performed at room temperature. Figure 4(a) shows the symmetric (002) and asymmetric (102) reflection of the HRXRD ω-scan rocking curves measured for both samples. The full width at half maximum (FWHM) values of the symmetry (002) ω-scan curve for MQW-on-PLA and MQW-on-PAT were found to be 296.2 arc sec and 270.8 arc sec, respectively, while those of the asymmetry (102) rocking curves for PLA and PAT were 312 arc sec and 248 arc sec, respectively. It has been reported that X-ray ω-scan curves on symmetric (002) planes are influenced by screw and mixed type dislocations, whereas ω-scan curves on asymmetric (102) planes are sensitive to edge type dislocations.[18,20] Based on these results, we were able to confirm that the material quality in MQW-on-PAT is improved compared to that in MQW-on-PLA due to a reduction of threading dislocations. Figure 4(b) exhibits the PL lifetime at room-temperature for MQW-on-PAT and MQW-on-PLA, as measured by TRPL. The excitation wavelength was chosen to be 385 nm using a frequency-doubled, femto-second Ti:sapphire laser, so that only the MQW regions would be excited. From the TRPL experiments, we found that the lifetimes are 3.7 ns and 3.1 ns for MQW-on-PAT and MQW-on-PLA, respectively. Since the PL lifetime of the InGaN MQWs at room-temperature may be mostly determined by the nonradiative recombination processes, the measured lifetime is strongly related to the material quality of the samples grown on different substrates. Therefore, these supporting experimental results are in good agreement with our analysis results.

Finally, it is worth noting that our proposed analysis method has several advantages over conventional methods that are based on the rate equation, as follows: (i) by using simple excitation power-dependence PL experiments, the IQE and each recombination process at arbitrary excitation power can be unambiguously determined without any knowledge of A, B, and C coefficients in the conventional rate equation. Note that P_{laser} and I_{PL} are exactly known from the excitation power-dependence PL experiment and one fitting parameter (P_2) can be easily fitted from the relationship between P_{laser} and I_{PL}. (ii) The fitting parameters (P_1, P_2, and P_3) are utilized to quantitatively calculate An, Bn^2, and Cn^3 in the conventional rate equation without any assumption about any of the recombination coefficients; consequently, the radiative optical properties (i.e., increase of light out power and relative recombination processes) and material quality (defect-related recombination process) of LEDs can be analyzed.

In summary, we have proposed a simple analysis method to calculate the IQE and relative carrier recombination ratios in LEDs. Based on our method, we conducted power-dependence PL experiments to calculate the IQE values of InGaN/GaN MQWs grown on patterned sapphire and planar sapphire substrates. We determined IQE values of 82% and 68% for MQW-on-PAT and MQW-on-PLA, respectively, using our proposed model. Furthermore, we were able to obtain the relative fitting parameters P_1, P_2, and P_3, which are associated with the SRH recombination rate, the radiative recombination rate, and the Auger recombination (and/or carrier overflow) rate, respectively, without any requirement of knowledge or assumptions about the values of the A, B, and C coefficients, unlike cases in which the conventional rate equation is used. Our results, obtained using a simple analysis method, are very consistent with our experimental data results from HRXRD and TRPL.

This work was supported by WCU Program (No. R31-2008-000-10071-0) of the Ministry of Education, the Industrial Strategic Technology Development Program (10041878) of the Ministry of Knowledge Economy, KAIST EEWS Initiative, and GRC project of KAIST Institute for the NanoCentury.

[1]E. F. Schubert and J. K. Kim, Science **308**, 1274 (2005).
[2]J. Piprek, Phys. Status Solidi A **207**, 2217 (2010).
[3]Y. C. Shen, G. O. Mueller, S. Watanabe, N. F. Gardner, A. Munkholm, and M. R. Krames, Appl. Phys. Lett. **91**, 141101 (2007).
[4]C. Xu, T. Yu, J. Yan, Z. Yang, X. Li, Y. Tao, X. Fu, Z. Chen, and C. Zhang, Phys. Status Solidi C **9**, 757 (2012).
[5]M. H. Kim, M. F. Schubert, Q. Dai, J. K. Kim, E. F. Schubert, J. Piprek, and Y. Park, Appl. Phys. Lett. **91**, 183507 (2007).
[6]X. Li, X. Ni, J. Lee, M. Wu, Ü. Özgür, H. Morkoç, T. Paskova, G. Mulholland, and K. R. Evans, Appl. Phys. Lett. **95**, 121107 (2009).
[7]T. Fleck, M. Schmidt, and C. Klingshirm, Phys. Status Solidi A **198**, 248 (2003).
[8]H. Gauck, T. H. Gfroerer, M. J. Renn, E. A. Cornell, and K. A. Bertness, Appl. Phys. A: Mater. Sci. Process. **64**, 143 (1997).
[9]R. K. Ahrenkiel, Solid-State Electron. **35**, 239 (1992).
[10]S. Watanabe, N. Yamada, M. Nagashima, Y. Ueki, C. Sasaki, Y. Yamada, T. Taguchi, K. Tadatomo, H. Okagawa, and H. Kudo, Appl. Phys. Lett. **83**, 4906 (2003).
[11]H. Kressel and J. K. Butler, *Semiconductor Lasers and Heterojunction LEDs* (Academic Press, New York, 1977).
[12]H. C. Casey, Jr. and M. B. Panish, *Heterostructure Lasers* (Academic Press, New York, 1978).
[13]J. Hader, J. V. Moloney, and S. W. Koch, Appl. Phys. Lett. **96**, 221106 (2010).
[14]A. David and N. F. Gardner, Appl. Phys. Lett. **97**, 193508 (2010).
[15]E. Kioupakis, Q. Yan, and C. G. Van de Walle, Appl. Phys. Lett. **101**, 231107 (2012).
[16]G.-B. Lin, D. Meyaard, J. H. Cho, E. F. Schubert, and H. W. Shim, Appl. Phys. Lett. **100**, 161106 (2012).
[17]M. F. Schubert, S. Chhajed, J. K. Kim, and E. F. Schubert, Appl. Phys. Lett. **91**, 231114 (2007).
[18]J.-H. Lee, J. T. Oh, Y. C. Kim, and J.-H. Lee, IEEE Photon. Technol. Lett. **20**, 1563 (2008).
[19]J. Yan, T. J. Yu, X. B. Li, B. Tao, and C. L. Xu, J. Appl. Phys. **110**, 073102 (2011).
[20]K. S. Lee, H. S. Kwack, J. S. Hwang, T. M. Rho, Y. H. Cho, J. H. Lee, Y. C. Kim, and C. S. Kim, J. Appl. Phys. **107**, 103506 (2010).